

## Conditions for Bound States in a Superconductor with a Magnetic Impurity\*

MICHAEL FOWLER AND KAZUMI MAKI†

*Department of Physics, University of Toronto, Toronto, Canada*

(Received 19 July 1967)

Using analytic continuation techniques recently developed for the normal-metal Kondo effect, we examine the structure of Suhl's scattering amplitudes in a superconductor. It is found that there are no bound states (poles in the energy gap) unless the Kondo coupling is stronger than the Cooper pairing force, i.e.,  $T_K > T_{c0}$ . The positions of the bound-state poles are given as a function of coupling strength and temperature. The poles always stay on the real axis.

### 1. INTRODUCTION

IT is well known that a magnetic impurity in a normal metal causes resonant spin-dependent scattering of conduction electrons at low temperatures.<sup>1</sup> The resulting localized variation in spin density lowers the ground-state energy of the system. This phenomenon is often referred to as a bound state,<sup>2</sup> although scattering-matrix theorists prefer to reserve that term for single-particle states corresponding to a real energy not lying in a continuum.<sup>3</sup> In the following, we use the words "bound state" in the latter sense only. Recent theoretical work on magnetic impurities in superconductors<sup>4,5</sup> suggests that here the situation is clear cut—switching on the interaction potential can cause the scattering matrix to have a pole in the energy gap. This is a bona fide bound state from any point of view, analogous, for example, to that associated with a single acceptor impurity in a semiconductor.

Recently, one of us has generalized Suhl's equations to the superconducting case,<sup>4</sup> and from an examination of the singularities of the scattering amplitudes certain conclusions about the existence of bound states were drawn. Unfortunately, some points concerning the analytic structure of the amplitudes involved were treated wrongly,<sup>6</sup> and the corrected treatment given below yields quite different criteria for the existence of bound states. The methods used in the present paper were first developed by one of us<sup>7</sup> to deal with Suhl's equations in a normal metal, but formally the solution for a superconductor is almost identical. The sheet structure of the singularities differs in an interesting

way from the normal case, as explained in Sec. 2; however, it goes over smoothly to the normal configuration as the gap becomes zero.

Physically, the conclusions reached are that there is no bound state until the Kondo temperature  $T_K$  [ $T_K = (2\gamma/\pi)De^{-1/\rho J}$ ,  $\gamma = 1.78$ , a measure of the impurity binding strength] reaches  $T_{c0}$ , the superconducting transition temperature. As  $T_K$  increases through  $T_{c0}$ , two poles enter the physical sheet symmetrically at opposite ends of the gap and move into the gap. This seems physically reasonable because the magnetic pairing force is, loosely speaking, competing with the Cooper pairing forces.<sup>8</sup>

One amusing feature is that as  $T_K$  is further increased, the poles move towards the center of the gap and then, for zero temperature, remain coincident there over a finite range of  $T_K$ . This is a reflection of the Fermi function, and except for a single value of  $T_K$  [i.e.,  $T_K = T_{c0} \exp(\frac{1}{2}\pi\sqrt{3})$ ] raising the temperature causes the poles to separate, the separation being linear in  $T$  for small  $T$ .

For very high values of  $T_K$ , the poles move asymptotically towards the ends of the gap, each pole approaching the end at which the other pole originated. For no values of  $T_K$  do the poles move off the real axis. However, if the BCS density of states is "rounded off" as it would be in a real alloy with magnetic impurities, for sufficiently high  $T_K$ , the bound-state poles go beyond the end of the gap onto the unphysical sheet, causing resonance scattering in the continuum. The precise form of the solution in this case depends strongly on the detailed shape of the assumed density of states, and we have so far been unable to extend our analysis to this case in a satisfactory fashion.

### 2. SOLUTION OF DISPERSION EQUATIONS FOR A SUPERCONDUCTOR

There are four possible scattering modes in this system, corresponding to spin-flip and non-spin-flip scattering, bearing in mind that a particle can scatter into a particle as well as into a hole. One of us<sup>4</sup> has derived scattering equations for the amplitudes con-

<sup>8</sup> We should perhaps point out that the bound state described recently by Hone and by Soda *et al.* (Ref. 5) is not simply related to the above bound state. In our terminology, they have calculated the ground-state energy of the total system in the presence of a single magnetic impurity, while we are interested in the single-particle energy spectrum of the system.

\* Supported in part by the National Research Council of Canada.

† On leave of absence from the Department of Physics, University of California, La Jolla, and from the Research Institute for Mathematical Sciences, Kyoto University, Kyoto, Japan.

<sup>1</sup> J. Kondo, *Progr. Theoret. Phys. (Kyoto)* **32**, 37 (1964).

<sup>2</sup> Y. Nagaoka, *Phys. Rev.* **138**, A1112 (1965); K. Yoshida, *ibid.* **147**, 223 (1966); A. J. Heeger and M. A. Jensen, *Phys. Rev. Letters* **18**, 488 (1967).

<sup>3</sup> For a complete summary, see H. Suhl, *Varenna lectures*, 1966 (to be published).

<sup>4</sup> K. Maki, *Phys. Rev.* **153**, 428 (1967).

<sup>5</sup> See also T. Soda, T. Matsuura, and Y. Nagaoka (Tokyo University of Education) and also report by D. Hone (University of Pennsylvania).

<sup>6</sup> In Ref. 4, conditions were found for zeros of  $S\tau^{-1}$ . These were assumed to correspond to poles in  $\tau$ . However, in the present work, it becomes obvious that  $S$ ,  $\tau$  have poles at the same points as in the normal case and  $S\tau^{-1}$  is well behaved at these points.

<sup>7</sup> M. Fowler, *Phys. Rev.* **160**, 463 (1967).

cerned under the usual assumption that only single-particle intermediate states are considered. The result is [Eq. 2(a) of Ref. 4]

$$t_{\pm}(z) = \int_{-D}^D \rho \frac{dx}{z-x} (|t_{\pm}|^2 + (3/16) |\tau_{\pm}|^2) (g \pm f) + \sum \frac{a_{\pm i}}{z-z_i} \quad (2.1)$$

$$\tau_{\pm}(z) = J + \int_{-D}^D \rho \frac{dx}{z-x} (t_{\pm}^* \tau_{\pm} + t_{\pm} \tau_{\pm}^* - \tanh \frac{\beta}{2} \beta x \times |\tau_{\pm}|^2) (g \pm f) + \sum \frac{b_{\pm i}}{z-z_i} \quad (2.2)$$

Here  $D$  is a cutoff energy of order  $\epsilon_F$ ,  $\rho$  is a constant,

$$g(z) = \text{Re} |z/(z^2 - \Delta^2)^{1/2}|, f(z) = \text{Re} |\Delta/(z^2 - \Delta^2)^{1/2}|,$$

$2\Delta$  being the BCS energy gap as usual; for the precise definitions of  $t_{\pm}$ ,  $\tau_{\pm}$ , see Ref. 4. The difference between (2.1), (2.2), and Suhl's equations for a normal metal is that Suhl's parabolic density of states is replaced by a BCS density  $\rho(g \pm f)$ . (Also, there is a factor of 4 difference in the definition of  $\tau$ .)

Since  $\rho(g \pm f)$  is identically zero in the gap  $(-\Delta, \Delta)$ , it is clear by inspection of (2.1), (2.2) that  $t$ ,  $\tau$  have cuts along the real axis from  $-D$  to  $-\Delta$  and from  $\Delta$  to  $D$ , and no other singularities on the physical sheet, apart from the pole terms for which  $a_{\pm i}$ ,  $b_{\pm i}$  are real and the  $z_i$  are real with  $|z_i| < \Delta$ . These terms were missing in the original equations, but are necessary to describe the bound state in a consistent way.

The pole terms represent possible bound states having energies in the gap. These should have been included in Eq. (29) of Ref. 4. They arise because if the full Hamiltonian has eigenstates with energies in  $(-\Delta, \Delta)$ , clearly the set  $|n\rangle$  [Ref. 4, Eq. (20)] of eigenstates of the full Hamiltonian having energies outside  $(-\Delta, \Delta)$  can no longer be a complete set, and inclusion of the bound eigenstates in the set gives the pole terms.

For definiteness, consider the coupled equation for  $t_+(z)$  and  $\tau_+(z)$ . We introduce two analytic functions  $t_1(z)$  and  $t_2(z)$  [also  $\tau_1(z)$  and  $\tau_2(z)$ ] equal to  $t_+(z)$  on the first sheet (that is, the physical sheet) and the second sheet, respectively. As  $t_1(z)$  has a discontinuity along the real axis for  $[-D, -\Delta]$  and for  $[\Delta, D]$ ,  $t_2(z)$  is the analytic continuation of  $t_1(z)$  onto the second sheet through this discontinuity. Hence for real  $x$

$$\lim_{\epsilon \rightarrow 0} t_2(x+i\epsilon) = \lim_{\epsilon' \rightarrow 0} t_1(x-i\epsilon') \quad \text{for } D > |x| > \Delta. \quad (2.3)$$

Furthermore, since the discontinuity across the real axis is pure imaginary, it follows that  $t_1(x) = t_2^*(x)$  for real  $x$ , and  $|t_+|^2$  in (2.1) can be written as  $t_1(x)t_2(x)$ . Hence  $|t_+|^2$  can be analytically continued into the complex plane in the form  $t_1(z)t_2(z)$ . It is interesting to notice that  $t_1(z)t_2(z)$  is analytic in the whole complex plane except for possible poles, whereas  $t_1(z)$  and  $t_2(z)$

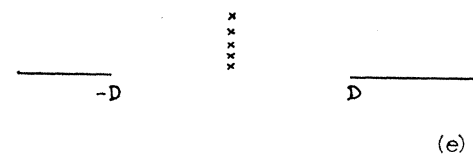
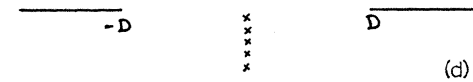
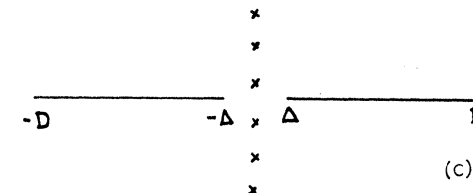
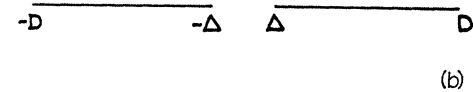
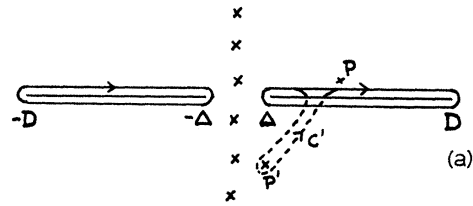


FIG. 1(a). Contour of integration and singularities of the integrand for  $G(z)$  (2.7). The pole  $P$  is at  $x=z$ . Analytic continuation in  $z$  is given simply by moving the pole  $P$  around. If  $P$  goes through the cut onto the second sheet to a point  $P'$ , the contour is dragged along ( $C'$  in figure). If  $P$  remains on the physical sheet, it is unnecessary to deform  $C$ . (b) Singularities of  $G(z)$  for  $z$  on the physical sheet. (c) Singularities of  $G(z)$  on the unphysical sheet. If  $P$  moves in the  $x$ -plane towards the pole of  $\tanh \beta x/2$  the contour  $C'$  is trapped, giving rise to a pole in  $G(z)$  at this point. (d) Singularity structure of  $G_R(z)$  in the normal case. (e) Singularity structure of  $G_A(z)$  in the normal case.

have the cuts mentioned above. This is a consequence of the fact that the BCS density of states gives rise to cuts of square root type so that only two sheets are involved.

Writing  $S(x) = 1 + 2\pi i \rho [(x+\Delta)/(x-\Delta)]^{1/2} t_1(x)$ , it is easy to derive unitarity equations analogous to (4.3) and (4.4) of Ref. 7.

$$S_1(x)S_2(x) + \frac{3}{4}\pi^2 \rho^2 [(x+\Delta)/(x-\Delta)] \tau_1(x)\tau_2(x) = 1, \quad (2.4)$$

$$\tau_1(x)S_2(x) - \tau_2(x)S_1(x) = -\pi i \rho [(x+\Delta)/(x-\Delta)]^{1/2} \tanh(\beta x/2) \tau_1(x)\tau_2(x). \quad (2.5)$$

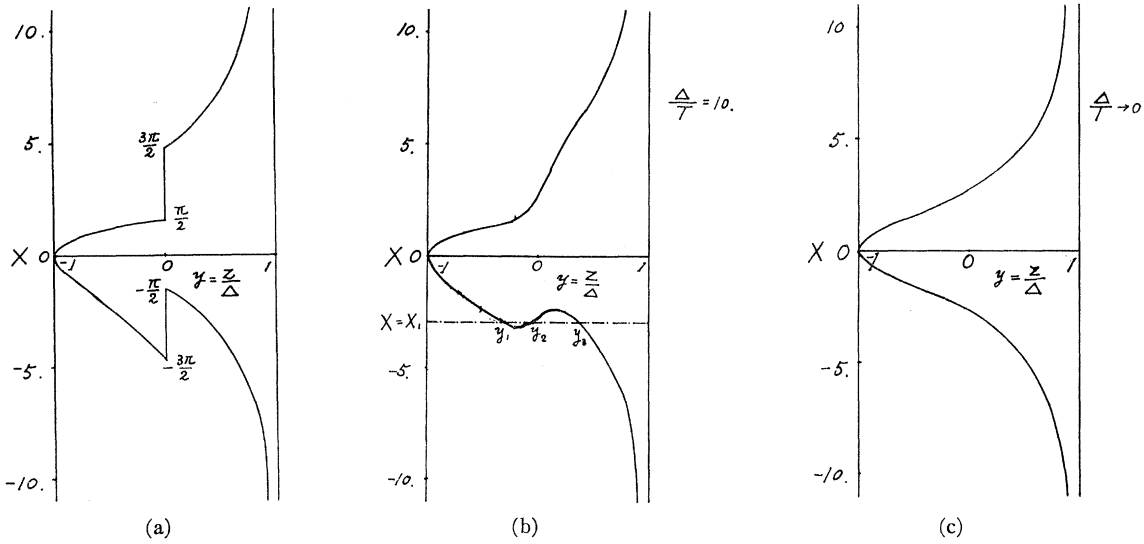


FIG. 2(a). Positions of poles of the scattering amplitudes  $t_+$ ,  $\tau_+$  plotted against the Kondo temperature for  $T=0$ . (b) Positions of poles when  $T=0.1\Delta$ . (c) Position of pole for  $T \lesssim \Delta$ . For  $0.9\Delta < T < \Delta$  deviations from this curve are too small ( $\sim 1\%$ ) to be plotted on this scale.

Defining  $G(x) = S(x)/\tau(x)$  gives

$$G_2(x) - G_1(x) = -\pi i \rho [(x+\Delta)/(x-\Delta)]^{1/2} \tanh(\beta x/2). \tag{2.6}$$

On the physical sheet,  $G$  has cuts from  $-D$  to  $-\Delta$  and from  $\Delta$  to  $D$ . At infinity,  $S=1$  and  $\tau=J$  from inspection of (2.1), (2.2) so  $G=1/J$ . Hence

$$G(z) = J^{-1} - \frac{1}{2} \int_c (z-x)^{-1} \rho [(x+\Delta)/(x-\Delta)]^{1/2} \tanh(\beta x/2). \tag{2.7}$$

For computational purposes, the integration can be taken along the real axis from  $-D$  to  $-\Delta$  and  $\Delta$  to  $D$ . To get a picture of the analytic structure of  $G$ , we take the contour around the two cuts as in Fig. 1(a). On the physical sheet, the only singularities of  $G$  are the real axis cuts [Fig. 1(b)]. Continuing onto the unphysical sheet in  $z$  [Fig. 1(c)] the contour of integration is dragged along and there is a singularity whenever it is "pinched" against a pole of  $\tanh \beta x/2$ . Hence on the unphysical sheet  $G$  has the real axis cuts, plus the singularities of  $\tanh \beta x/2$ . This is of course clear from (2.6). It is instructive to compare this singularity structure with that of  $G_R(z)$ ,  $G_A(z)$  in the normal case [Figs. 1(d), 1(e)]. How does one go to the other as  $\Delta$  goes to zero? The answer is that for  $\Delta \neq 0$  the "natural" continuation of  $G(z)$  from the upper into the lower half plane is across the real axis through the gap. For  $\Delta$  zero, one is forced in continuing  $G(z)$  into the lower half plane to go through the cut onto the second sheet. In other words, at  $\Delta=0$ , both sheets of  $G(z)$  have been cut in two along the real axis and the top half of one sheet now continues into the bottom half of the other, giving the familiar digamma structure. (It should be mentioned that we never consider continuation across

the real axis beyond  $D$ . This can be done, but adds nothing new and is a less "natural" definition of a single sheet, because the interesting analytic structure is much closer to the origin.) Terms such as  $(D+x/D-x)^{1/2}$  have also been omitted from (2.6) because they are practically unity in the region of interest.

Solving (2.4) and (2.5) using (2.6) gives

$$\tau_1(x)\tau_2(x) = \frac{1}{G_1(x)G_2(x) + \frac{3}{4}\pi^2\rho^2[(x+\Delta)/(x-\Delta)]}, \tag{2.8}$$

$$S_1(x)S_2(x) = \frac{G_1(x)G_2(x)}{G_1(x)G_2(x) + \frac{3}{4}\pi^2\rho^2[(x+\Delta)/(x-\Delta)]}. \tag{2.9}$$

From (2.8) and (2.9) it follows that poles of  $\tau_+$ ,  $S_+$  are given by

$$G_1(x)G_2(x) + \frac{3}{4}\pi^2\rho^2[(x+\Delta)/(x-\Delta)] = 0. \tag{2.10}$$

Writing  $X = \ln T_K/T_{c0}$  [where  $T_K = (2\gamma/\pi)De^{-1/\rho J}$  and  $T_{c0}$  is the critical temperature of the superconductor]  $y = x/\Delta$ ,  $\alpha = \Delta/T$ , this condition (for spin  $S$ ) is easily seen to be

$$[X + A_+(y)]\{X + A_+(y) - \pi[(1+y)/(1-y)]^{1/2} \times \tanh[(\alpha/2)y]\} - S(S+1)\pi^2[(1+y)/(1-y)] = 0, \tag{2.11}$$

where

$$A_+(y) = y(y+1) \int_1^\infty dx/(x^2-1)^{1/2} \frac{\tanh(\frac{1}{2}\alpha x)}{x^2-y^2}. \tag{2.12}$$

This integral can be evaluated explicitly for  $T \ll \Delta$  and  $T \gg \Delta$  (this is done in the Appendix).

Hence we can plot now the position of poles of the scattering amplitude behaves as a function of  $X$ .  $X$  is just a measure of the strength of the Kondo binding

relative to the Cooper binding, i.e.,

$$X = \ln(T_K/T_{c0}) = \ln(D/\omega_D) + \rho^{-1}(|g|^{-1} - J^{-1}),$$

where  $\omega_D$  is the Debye cutoff frequency and  $|g|$  is the pairing interaction strength. Figure 2 graphs the  $y-X$  dependence for various temperatures.

From an examination of Fig. 2, we can determine when the poles are on the physical sheet. Consider, for example, Fig. 2(b) and suppose the strength is given by the line  $X=X_1$ . Then there are three poles of  $\tau$  on the real axis at the points  $y_1, y_2, y_3$ . If the Kondo coupling is weakened, the line  $X=X_1$  moves downwards, and the poles  $y_1, y_2$  come together and then go into the complex plane symmetrically. For an arbitrarily weak Kondo coupling,  $y_1$  and  $y_2$  will be in the complex plane. This is physically unreasonable unless  $y_1, y_2$  are on the unphysical sheet for otherwise an arbitrarily weak interaction will cause a breakdown of causality. Hence we take it that for  $X=X_1$ ,  $y_1, y_2$  are on the unphysical sheet, (i.e., on the second sheet). Now increasing the strength  $X$ ,  $y_2, y_3$  become coincident and then complex. This can only happen if they are on the same sheets so the conclusion is that for  $X=X_1$  all three poles are on the unphysical sheet. If  $X$  is increased to zero, the pole  $y_1$  moves to the end of the gap and comes through the cut onto the physical sheet. It then represents a zero energy bound state. At this point  $T_K=T_{c0}$ . Further increase in  $T_K$  causes the bound state pole to traverse the gap, as is easily seen in Fig. 2. The complex poles  $y_2, y_3$  can never get onto the physical sheet because to do so they would have to go through the cuts, and hence become real again. However, the curves in Fig. 2 give all possible real values of pole position. For high temperatures  $T \lesssim T_{c0}$ , no horizontal line cuts the curve at three points. However, it is clear that the bound state poles are in the physical sheet for  $T_K > T_{c0}$  since the system varies smoothly with increase of temperature from  $T \ll T_{c0}$  to  $T \lesssim T_{c0}$ .

The poles of the amplitudes  $t_-, \tau_-$  defined by Maki are given by curves identical with those of Fig. 2 but with the sign changed along the horizontal axis. Thus when the  $y_1$  of  $t_+$  enters the physical sheet at  $-\Delta$ , a pole  $y_1' = -y_1$  of  $t_-$  enters at  $\Delta$ . The full non-spin-flip amplitude  $t = t_+ + t_-$  defined by Maki thus has its real poles always symmetrically placed about the center of the gap.

### 3. CONCLUSION

By using analytic continuation techniques, we have solved the dispersion equation of the scattering matrix for a quasiparticle in a superconductor interacting with a magnetic impurity. We find that (a) if  $T_K < T_{c0}$ , the pole appears only in the second sheet (i.e., no bound state in the energy gap); (b) if  $T_K > T_{c0}$ , the bound-state pole appears in the first sheet in the energy gap (i.e. a quasiparticle is trapped around the impurity atom). This general feature is independent of the tem-

perature (as long as  $T < T_{c0}$ ) or of the magnitude of spin  $S$  of the localized moment, although the position of the pole wanders around as the temperature increases. Note that this pole appears both in the spin-flip and in the non-spin-flip scattering amplitudes. In order to discuss the feasibility of experimentally observing this bound state, it is necessary to generalize the present analysis to the case of finite impurity concentration. The formal procedures used in Ref. 4 have to be followed. The most important effect of a finite concentration of magnetic impurities is that the density of states [i.e.,  $g(x)$  and  $f(x)$ ] is drastically modified. Hence in order to reach a definite conclusion, more detailed analysis is required. However, we may expect that in the situation  $T_K \gg T_{c0}$ , there will be additional structure in the density of states at the energy of the bound state, which may affect various transport properties of the system. These problems will be left for a future study.

### APPENDIX

We present here the calculations involved in determining the location of the bound-state poles. The impurity spin is taken to be  $S$  throughout. The positions of the poles in  $\tau_1(z) \cdot \tau_2(z)$  are given by

$$\begin{aligned} ((J\rho)^{-1} - A_+(z)) \left( (J\rho)^{-1} - A_+(z) + i\pi \left( \frac{\Delta+z}{\Delta-z} \right)^{1/2} \tanh \frac{z}{2T} \right) \\ - \pi^2 S(S+1) \frac{\Delta+z}{\Delta-z} = 0, \quad (\text{A1}) \end{aligned}$$

where

$$A_+(z) = \frac{1}{2} \int_{-D}^D \frac{dx}{x-z} \left( \tanh \frac{x}{2T} \right) \text{Re} \left\{ \left( \frac{\Delta+x}{\Delta-x} \right)^{1/2} \right\}. \quad (\text{A2})$$

Equation (A1) can be rewritten

$$\begin{aligned} X_+ = \frac{1}{2} \pi \left( \frac{1+y}{1-y} \right)^{1/2} \{ [4S(S+1) + \tanh^2(\frac{1}{2}\alpha y)]^{1/2} \\ + \tanh(\frac{1}{2}\alpha y) \} - B_+(y), \quad (\text{A3}) \end{aligned}$$

$$\begin{aligned} X_- = -\frac{1}{2} \pi \left( \frac{1+y}{1-y} \right)^{1/2} \{ [4S(S+1) + \tanh^2(\frac{1}{2}\alpha y)]^{1/2} \\ - \tanh(\frac{1}{2}\alpha y) \} - B_+(y), \quad (\text{A4}) \end{aligned}$$

where

$$\begin{aligned} X_{\pm} = \ln T_K/T_{c0}, \quad y = z/\Delta, \quad \alpha = \Delta/T, \\ B_+(y) = (1+y)y \int_1^{\infty} dx (x^2-1)^{1/2} \frac{\tanh(\frac{1}{2}\alpha x)}{x^2-y^2}, \quad (\text{A5}) \end{aligned}$$

where we have made use of the relation

$$\begin{aligned} A_+(y) = \ln \frac{2D}{\Delta} \\ + z(z+\Delta) \int_1^{\infty} dx / (x^2-\Delta^2)^{1/2} \frac{\tanh(z/2T)}{x^2-z^2}. \quad (\text{A6}) \end{aligned}$$

Here  $X_+$  and  $X_-$  correspond to the two roots of (A1).

(a)  $T=0$ : In  $B_+(y)$  we first take  $T=0^\circ\text{K}$ . In this case (A5) reduces to

$$B_+(y) = (1+y)y \int_1^\infty \alpha x / (x^2-1)^{1/2} (x^2-y^2)^{-1} dx \\ = [(1+y)/(1-y)]^{1/2} \text{arcsiny}. \quad (\text{A7})$$

Substituting this expression in (A3) and (A4) we have

$$X_+ = [(1+y)/(1-y)]^{1/2} \{ \pi(S+1) + (y/|y|) \text{arcsiny} \}, \quad (\text{A8})$$

$$X_- = -[(1+y)/(1-y)]^{1/2} \{ \pi(S+1) - (y/|y|) \text{arcsiny} \}, \quad (\text{A9})$$

respectively, which are plotted in Fig. 2(a).

(b)  $T \ll T_{e0}$ : In this limit  $B_+(y)$  is given by

$$B_+(y) = (1+y)y \int_1^\infty dx / (x^2-1)^{1/2} \frac{1-2f(\alpha x)}{x^2-y^2} \\ = \left( \frac{1+y}{1-y} \right)^{1/2} \text{arcsiny} \\ - 2y(1+y) \int_1^\infty dx / (x^2-1)^{1/2} \frac{f(\alpha x)}{x^2-y^2}, \quad (\text{A10})$$

where  $f(E) = (1+e^E/T)^{-1}$ . Assuming  $\alpha(1-|y|) \gg 1$ ,

$$X_+ = \frac{1}{2}\pi [(1+y)/(1-y)]^{1/2} \{ [4S(S+1) + \tanh^2(\frac{1}{2}\alpha y)]^{1/2} + \tanh(\frac{1}{2}\alpha y) - (2/\pi) \text{arcsiny} \} + O[\exp(-\Delta/T)], \quad (\text{A14})$$

and

$$X_- = -\frac{1}{2}\pi [(1+y)/(1-y)]^{1/2} \{ [4S(S+1) + \tanh^2(\frac{1}{2}\alpha y)]^{1/2} - \tanh(\frac{1}{2}\alpha y) + (2/\pi) \text{arcsiny} \} + O[\exp(-\Delta/T)]. \quad (\text{A15})$$

(c)  $T \simeq T_{e0}$ : In the high-temperature region we have

$$B_+(x) = (1+y)y \int_1^\infty dx / (x^2-1)^{1/2} (x^2-y^2)^{-1} \sum_{n>0} \frac{\alpha x}{\pi^2(n+\frac{1}{2})^2 + (\frac{1}{2}\alpha x)^2} \\ = \alpha \sum_{n>0} (1+y)y \int_1^\infty dx / (x^2-1)^{1/2} \frac{x}{x^2-y^2} [\pi^2(n+\frac{1}{2})^2 + (\frac{1}{2}\alpha x)^2]^{-1} \\ = \alpha \sum_{n>0} (1+y)y \int_0^\infty \frac{dt}{t^2+1-y^2} [\pi^2(n+\frac{1}{2})^2 + (\frac{1}{2}\alpha)^2(t^2+1)]^{-1} \\ = \alpha y(1+y) \sum_{n>0} [\pi^2(n+\frac{1}{2})^2 + (\frac{1}{2}\alpha y)^2]^{-1} \int_0^\infty dt \left[ (t^2+1-y^2)^{-1} - \frac{(\frac{1}{2}\alpha)^2}{\pi^2(n+\frac{1}{2})^2 + (\frac{1}{2}\alpha)^2(t^2+1)} \right] \\ = \alpha y(1+y) \frac{1}{2}\pi \sum_{n>0} [\pi^2(n+\frac{1}{2})^2 + (\frac{1}{2}\alpha y)^2]^{-1} \{ (1-y^2)^{-1/2} - (\frac{1}{2}\alpha) [\pi^2(n+\frac{1}{2})^2 + (\frac{1}{2}\alpha)^2]^{-1/2} \} \\ = \frac{1}{2}\pi(1+y) \{ \tanh \frac{1}{2}\alpha y / (1-y^2)^{1/2} - \frac{1}{2}\alpha^2 y \sum_{n>0} [\pi^2(n+\frac{1}{2})^2 + (\frac{1}{2}\alpha y)^2]^{-1} [\pi^2(n+\frac{1}{2})^2 + (\frac{1}{2}\alpha)^2]^{-1/2} \} \\ \cong \frac{1}{2}\pi [(1+y)/(1-y)]^{1/2} \{ \tanh \frac{1}{2}\alpha y - \frac{1}{2}\alpha^2 y (1-y^2)^{1/2} [7\zeta(3)/\pi^3] - [31\zeta(5)/\pi^5] (\frac{1}{2}\alpha)^2 (y^2 + \frac{1}{2}) \}. \quad (\text{A16})$$

Finally, the positions of the pole are given by

$$X_+ = \frac{1}{2}\pi [(1+y)/(1-y)]^{1/2} \{ [4S(S+1) + \tanh^2(\frac{1}{2}\alpha y)]^{1/2} + y(1-y^2)^{1/2} [7\zeta(3)/2\pi^3] \alpha^2 + O(\alpha^4) \},$$

and

$$X_- = -\frac{1}{2}\pi [(1+y)/(1-y)]^{1/2} \{ [4S(S+1) + \tanh^2(\frac{1}{2}\alpha y)]^{1/2} - y(1-y^2)^{1/2} [7\zeta(3)/2\pi^3] \alpha^2 + O(\alpha^4) \}. \quad (\text{A17})$$

we transform the second term in (A10) as

$$\int_1^\infty \alpha x / (x^2-1)^{1/2} \frac{f(\alpha x)}{x^2-y^2} dx \\ \cong (2y)^{-1} \int_1^\infty \alpha x / (x^2-1)^{1/2} dx \\ \times [(x-y)^{-1} - (x+y)^{-1}] \exp(-\alpha x) \\ \cong (2y)^{-1} K_0(\alpha) [(1-y)^{-1} - (1+y)^{-1}]. \quad (\text{A11})$$

Combining this we have

$$B_+(y) = [(1+y)/(1-y)]^{1/2} \times [\text{arcsiny} - (2y/(1-y^2)^{1/2}) K_0(\Delta/T)] \quad (\text{A12})$$

or

$$B_+(y) = [(1+y)/(1-y)]^{1/2} \text{arcsiny} - O[\exp(-\Delta/T)].$$

On the other hand, if  $\alpha(1-|y|) \ll 1$ , a detailed treatment gives

$$B_+(y) = \frac{1}{2}\pi (2/1-y)^{1/2} [1 - 2 \exp(-\Delta/T)]. \quad (\text{A13})$$

Substituting the above expressions for  $B_+(y)$  in (A3) and (A4), we see that significant changes in the location of the poles occur only for poles close to  $z=0$ . Approximate expressions for  $X_+$  and  $X_-$  are now given by